ELSEVIER

Journal of Molecular Catalysis A: Chemical 182–183 (2002) 125–136

JOURNAL OF MOLECULAR CATALYSIS A: CHEMICAL

www.elsevier.com/locate/molcata

Design of catalytic sites at oxide surfaces by metal-complex attaching and molecular imprinting techniques

A. Suzuki, M. Tada, T. Sasaki, T. Shido, Y. Iwasawa*

Department of Chemistry, Graduate School of Science, The University of Tokyo, Hongo, Bunkyo-ku, Tokyo 113-0033, Japan

Received 31 August 2001; accepted 2 November 2001

Abstract

This paper attempts to summarize our recent studies on the chemical design and characterization of catalytic sites at oxide surfaces such as Nb monomer, dimer and monolayer on SiO_2, Rh dimers on SiO_2, TiO_2, Al_2O_3, and MgO, and Au nanoparticles on TiO_2(1 1 0), prepared by using suitable metal-complex precursors in a molecular scale. The paper also reports performances of new molecular imprinting catalysts, SiO_2 overlayers/α-Al_2O_3 and Rh–SiO_2 overlayers/SiO_2, designed by surface molecular imprinting techniques.

Keywords: Chemical design of catalyst surfaces; Active structures; Supported metal complexes; Molecular imprinting; Ethanol dehydrogenation; Ethene hydroformylation; Ester hydrolysis; Alkene hydrogenation; Niobium; Rhodium

1. Introduction

Selectivity in catalytic oxidation and acid–base reactions has been a long-term challenge in surface catalytic chemistry. While it has been recognized that promotion and control of the reactivity of adsorbed species and reaction intermediates at catalyst surfaces are critical in achieving the selectivity, this issue has not been adequately addressed and is a serious challenge to the field. It has been demonstrated that catalytic reactions are controlled by catalyst surface properties, but at the same time they are regulated by chemical interaction between reaction intermediate and co-adsorbate even when the interaction is very weak or undetectable [1–4]. The requirements and design of quantitative ensemble sizes also represent important but as yet unaddressed challenges [2,5].

Chemical design of a variety of active structures has been attempted to develop a new class of catalysts by metal-complex attaching and molecular imprinting techniques. Although the efforts on the design of excellent catalysis have been acutely difficult challenges, recently molecular-level catalyst preparation has become realistic on the basis of modern physical techniques and accumulated knowledge of oxide surfaces [2]. The new and distinct materials and chemistry prepared stepwise in a controllable manner by using metal-organic and -inorganic complexes as precursors provide an opportunity for the development of efficient catalytic molecularly organized surfaces. Understanding and controlling catalyst surfaces are the key issues for development of industrial catalysts, but supported metal and metal oxide surfaces are generally heterogeneous and complicated. The key factors of chemical design of supported catalyst surfaces are composition, structure, oxidation state, distribution, morphology, polarity, etc. which should be organized at the surface. In the development of new catalysts, new chemical

* Corresponding author. Fax: +81-3-5800-6892.
E-mail address: iwasawa@chem.s.u-tokyo.ac.jp (Y. Iwasawa).

1381-1169/02/$ – see front matter
PII: S1381-1169(01)00505-2

concepts regarding composition or structure are conceived. Characterization should be achieved for real active sites and adsorbed species that are discriminated from spectators which often coexist on the catalyst surfaces. Highly detailed picture of a mechanism evolves in situ observation and analysis [1,2].

The aim of this paper is to summarize our recent work on chemical design of catalytic sites at oxide surfaces by metal-complex attaching and molecular imprinting techniques, presenting previous typical examples of molecular-level preparation of active surface structures and also new performances of novel surface molecular imprinting catalysts.

2. Molecular-level catalyst preparation

Table 1 shows typical approaches to chemical design of active metal sites and ensembles on oxide surfaces by metal-organic and -inorganic complexes and clusters. Catalysts can be prepared by an approach which stems from the concept of surface organometallic chemistry to generate a well-defined coordination sphere around a metal atom on oxide support via a direct covalent bond between the metal and the metal oxide such as silica, alumina, or titania. For example, Basset and coworkers [6] reported a Re carbene complex supported on silica via the direct bonding. The supported Re carbene species was characterized by ^{1}H and ^{13}C NMR comparing the corresponding homogeneous Re carbene complex. The surface Re species was active for propene metathesis at room temperature. This catalyst preparation is classified to the first and second approaches among many approaches in Table 1 [7]. The complexes and clusters can be attached to oxide surfaces by selective reactions such as ligand–surface OH reactions, redox reactions and acid–base reactions. Designed structures can be obtained by surface synthesis and surface transformation starting from the initially attached species. Main elements inside cluster frameworks like $[Ru_6C]$ serve as promoters to affect the reactivity of metal sites sometimes remarkably [8]. Selective element replacement of cations at oxide surfaces by active metal atoms is also possible by using metal-inorganic complex and cluster; an example of the category 7 is $Pt(acac)_2$ and $[PtMo_6]$ on MgO, where surface Mg ions are selectively replaced by Pt ions to provide active catalysts for the selective dehydrogenation of propane, butane, and isobutene to the corresponding alkenes [9]. Recently, molecular imprinting catalysts have accepted attention to provide a new class of heterogeneous catalysts with shape selectivity and molecular recognition like enzymatic catalysis [10–16]. Well-defined surfaces of crystalline materials like oxide single crystals can be used as supports for metal complex precursors. When $Au(PPh_3)(NO_3)$ is deposited on $TiO_2(1\,1\,0)$ single crystal, $Au(PPh_3)(NO_3)$ is self-aggregated to large particles at 363 K, and hence subsequent calcination at 473 K forms large Au particles with about 3 nm height at the surface. In contrast, when the $TiO_2(1\,1\,0)$ surface is irradiated by UV light before the $Au(PPh_3)(NO_3)$ deposition, small and flat Au particles with <1 nm height and relatively uniform size distribution is found [17]. The catalysts reported in this study are classified to the first, second, and eighth approaches in Table 1, based on attachment of appropriate metal complexes on oxide surfaces followed by chemical treatments of the incipient attached metal complexes.

Table 1
Typical approaches to chemical design of active metal sites and ensembles on oxide surfaces by metal-organic and -inorganic complexes and clusters

1	Selective reactions of complexes and clusters with surface OH groups: (a) ligand–OH reactions, (b) redox reactions, (c) acid–base reactions
2	Surface synthesis and surface transformation
3	Electrostatic or electronic interaction at interface
4	Ship-in-a-bottle synthesis
5	Epitaxial growth of active structures
6	Promoters (on, inside, near and far)
7	Selective element-exchange at cation and anion sites of surfaces
8	Molecular imprinting
9	Definite surfaces of crystalline materials
10	Others

2.1. Nb monomer, dimer, and monolayer on SiO_2

The SiO_2-attached Nb monomer catalyst (**1**) with a four-coordinate structure in Fig. 1 was prepared by the use of $Nb(\eta^3\text{-}C_3H_5)_4$ as precursor and characterized by extended X-ray absorption fine structure (EXAFS), FT-IR, Raman, ESR, and XPS [2,3,7]. $Nb(\eta^3\text{-}C_3H_5)_4$ was reacted with surface OH groups of SiO_2, followed by stepwise treatments with H_2 and O_2. The Nb=O,

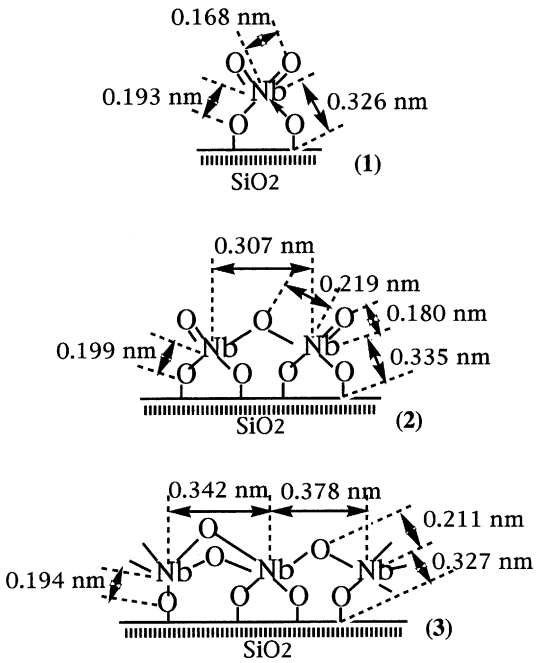

Fig. 1. The Nb monomer, dimer, and monolayer structures attached on SiO_2 surfaces.

Nb–O and Nb–Si interatomic distances in the catalyst (**1**) were determined to be 0.168, 0.193, and 0.326 nm, respectively, by EXAFS. No Nb–Nb bonding was observed by EXAFS, demonstrating that the Nb^{5+} ions are distributed as monomers on the SiO_2 surface.

Nb dimers on SiO_2 (**2**) in Fig. 1 can also be prepared by using a dimeric Nb precursor $[Nb(\eta^5\text{-}C_5H_5)H\text{-}\mu\text{-}(\eta^5,\eta^1\text{-}C_5H_4)]_2$ in the controllable step [18]. The first step of preparation of (**2**) was the reaction of the hydride ligand with surface silanols to form surface-attaching Nb dimers with the Nb–Nb, Nb–C, and Nb–O (surface) bond distances of 0.334, 0.243, and 0.201 nm, respectively. Then the obtained surface dimers were converted to the Nb dimer catalyst (**2**) by stepwise treatments with H_2 and O_2. The surface dimers (**2**) with a Nb–Nb distance of 0.307 nm were chemically bound to the SiO_2 surface at a Nb–Si interatomic distance of 0.335 nm through the interfacial Nb–O (surface) bond at 0.199 nm as shown in Fig. 1.

Further, the Nb monolayer on SiO_2 (**3**) in Fig. 1 can also be prepared by using Nb ethoxide $Nb(OC_2H_5)_5$ as precursor [2]. In the monolayer structure (**3**), there are two different Nb–Nb bonds at 0.342 and 0.378 nm. The Nb–Si interatomic distance was also determined to be 0.327 nm by EXAFS. The interfacial Nb–O bonds were similar to the other Nb structures (**1** and **2**).

2.2. Rh dimers on SiO_2, TiO_2, Al_2O_3, and MgO

Incipient attached Rh dimers were prepared by reaction of *trans*-$[(RhCp^*CH_3)_2(\mu\text{-}CH_2)_2]$ (Cp^* = pentamethylcyclopentadienyl) with surface OH groups of SiO_2, TiO_2, Al_2O_3, or MgO in pentane at ambient temperature under 99.9999% He or 99.9999% Ar. The incipient Rh dimer on SiO_2 was converted to the Rh dimer species (**4**) in Fig. 2 by stepwise transformation at the surface [19]. Each step for the transformation was characterized by FT-IR (use of deuterium-labeled Rh dimer precursor) and EXAFS. The Rh dimer/SiO_2 (**4**) was employed as catalyst for ethene hydroformylation. The dimer (**4**) with an acyl ligand is favorable as a catalyst for ethene hydroformylation because the Rh acyl species is a reaction intermediate for the hydroformylation. Thus, we succeeded in the design of the catalytic site with the reaction intermediate. The Rh–Rh bond was observed at 0.270 nm by EXAFS. In the dimer (**4**), one Rh atom with the acyl ligand may work as the reaction site, while another Rh atom may promote the Rh reaction site as a promoter. Rh dimer catalysts were also prepared for TiO_2, Al_2O_3, and MgO, but the produced structures were different from each other. Proposed Rh structures (**6**–**9**) on the oxide surfaces characterized by FT-IR and EXAFS are shown in Fig. 3 [20]. The Rh loadings were controlled to be 0.1–0.2 dimers nm^{-2} for SiO_2, 0.6–1.2 dimers nm^{-2} for TiO_2, 0.3–0.6 dimers nm^{-2} for Al_2O_3, and 0.2–0.6 dimers nm^{-2} for MgO to avoid undesired aggregation of Rh species at the surface.

2.3. Molecular imprinting catalysts

Preparation steps for a molecular imprinting catalyst (**10**) for ester hydrolysis are shown in Fig. 4 [16,21]. Diethyl benzylphosphonate was chosen as a template for the preparation of the molecular imprinting catalyst (**10**). Diethyl benzylphosphonate vapor was admitted to $\alpha\text{-}Al_2O_3$ surface (surface area: 12 $m^2\,g^{-1}$) at room temperature. The $\alpha\text{-}Al_2O_3$ was heated at 673 K for 2 h under vacuum before use as support. The amount

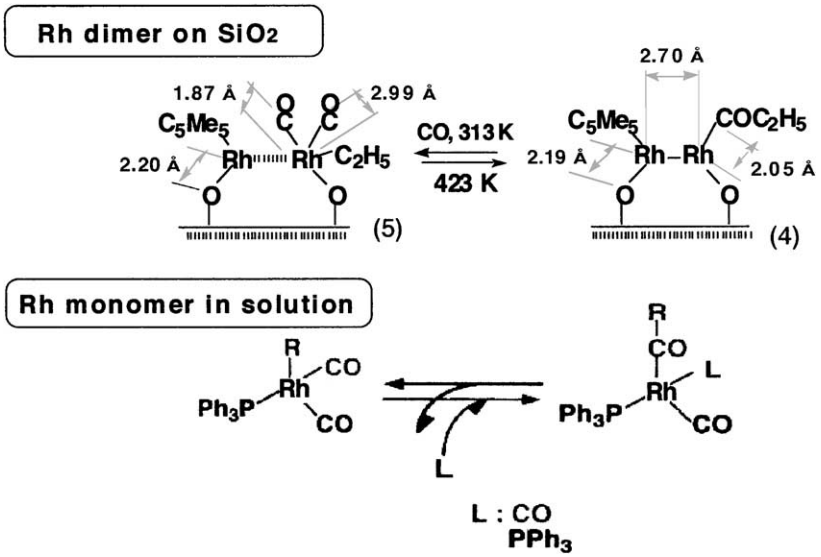

Fig. 2. Transformations of the Rh dimer on SiO_2 and the Rh monomer in solution for CO insertion and decarbonylation.

of the template was 5.4 mg per 1 g of the alumina. The obtained sample was exposed to $Si(OCH_3)_4$ vapor at 338 K, followed by hydrolysis with H_2O vapor at 423 K. The amount of the deposited $Si(OCH_3)_4$ for each cycle was controlled to be 1.8×10^{-3} mol per 1 g of alumina. The CVD-hydrolysis cycles were repeated 10 times to fully cover the alumina surface by the SiO_2 overlayers. Then the template molecules were removed by refluxing ethanol for 30 h. The template molecules in the sample after the CVD-hydrolysis cycles remained unchanged in the structure at the alumina surface as proved by UV–Vis spectroscopy. The amount of phosphorous atoms in the samples was determined by ICP mass spectrometry. The P amounts after deposition and extraction were 22 and 3 μmol g_{cat}^{-1}. The results demonstrate that 86% of the template was

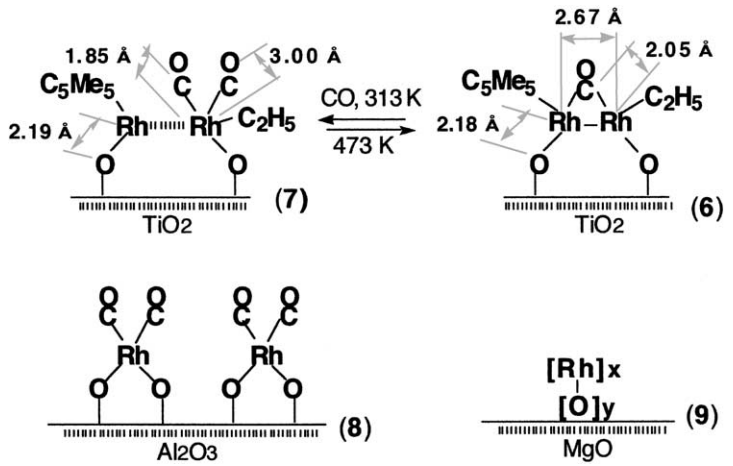

Fig. 3. Surface Rh structures attached on TiO_2, Al_2O_3, and MgO.

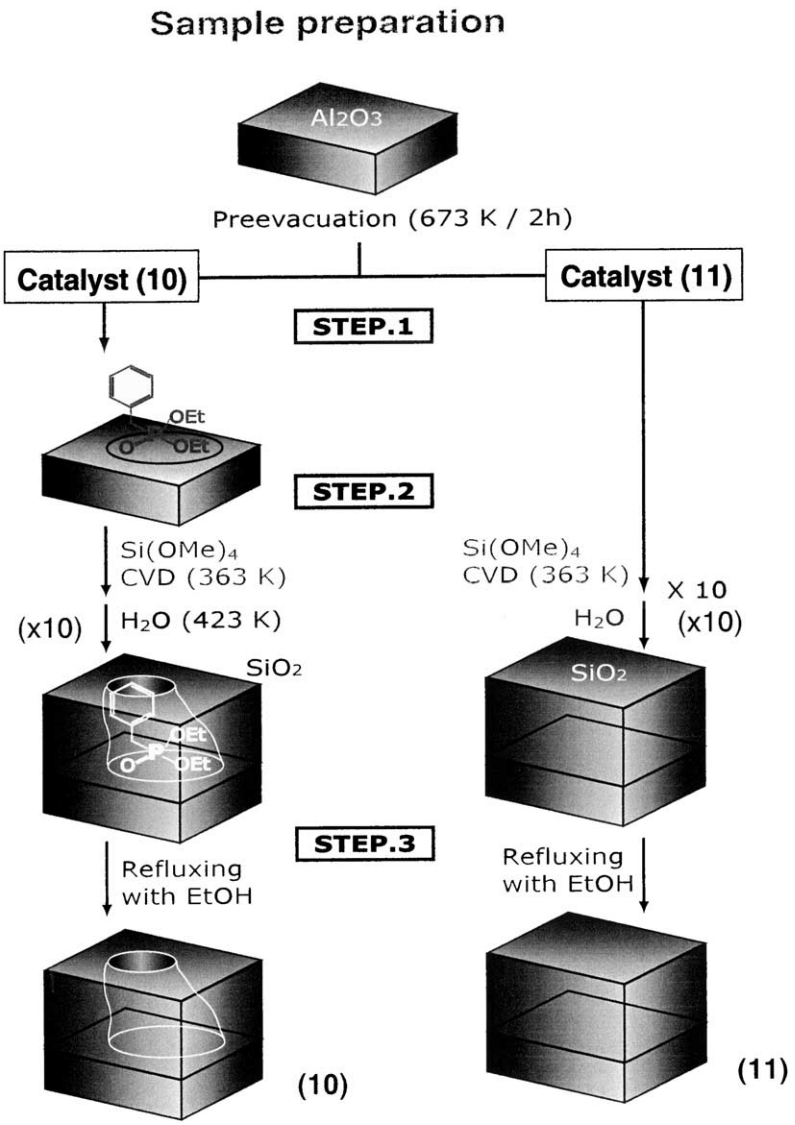

Fig. 4. Preparation steps for the imprinted catalyst (**10**) and the reference supported catalyst (**11**).

removed by extraction, and as a result the number of pores was assumed to be 19 μmol g_{cat}^{-1}, which corresponds to a surface density of 0.52 nm^{-2}.

A catalyst prepared in a similar way but without the template is denoted as catalyst (**11**). The number of CVD-hydrolysis cycles was changed in the range 1–10 to examine the sufficient number of cycles for SiO_2 overlayers to completely cover the alumina surface. Ten cycles were necessary to fully cover the alumina surface judging from suppression of the intrinsic Lewis acidity of the alumina surface.

We have also prepared molecular imprinting catalysts with Rh complexes as active sites for alkene hydrogenation [22]. The detail of the preparation will be reported elsewhere [23], but it is briefly summarized. $P(OCH_3)_3$ was chosen as template, where the $P(OCH_3)_3$ molecule can be regarded as an analog to the half-hydrogenated intermediate for the

hydrogenation of internal alkenes. At first, $Rh_2Cl_2(CO)_4$ was supported on TiO_2 (P25; 50 $m^2\,g^{-1}$) and SiO_2 (OX50; 50 $m^2\,g^{-1}$). The Rh loadings were controlled to be 0.1–0.4 wt.%. Then, a given amount of $P(OCH_3)_3$ template molecules was coordinated to the supported Rh atoms, accompanied with complete loss of the CO ligands. Finally, the obtained samples were exposed to $Si(OCH_3)_4$ and H_2O vapors at room temperature, followed by hydrolysis at 348 K and evacuation at 363 K. The amount of $Si(OCH_3)_4$ was regulated to be equivalent to three SiO_2 layers. The SiO_2 overlayers (surface matrix) were characterized by solid-state MAS ^{29}Si NMR, which exhibits three distinct peaks for Si(4OSi), Si(3OSi), and Si(2OSi). The well-separated three-peak feature was entirely different from the ill-defined feature for usual SiO_2 gels. The samples formed at each preparation step were characterized by chemical analysis, FT-IR, ICP mass spectroscopy, solid-state MAS ^{29}Si and ^{31}P NMR, XRF, XPS, and EXAFS [23]. The obtained imprinted samples were stocked in Schlenk tubes in refrigerator until use as catalysts.

3. Catalytic performances and reaction mechanisms

3.1. Nb catalysts

The Nb monomer catalyst (**1**) exhibited high activity and selectivity for the dehydrogenation of ethanol to form acetaldehyde and H_2 in the temperature range 423–523 K as shown in Table 2 [2]. The activity was much higher than that of a usual impregnation

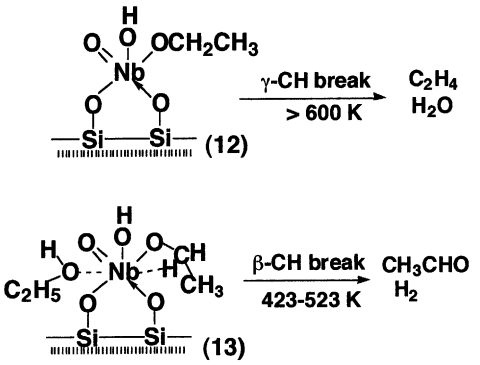

Fig. 5. Switchover of the reaction paths by weak ethanol coordination.

Nb catalyst and the selectivity was as high as 95–100%. The dehydrogenation reaction proceeded via the Nb-ethoxide intermediate (**12**), but the intermediate was very stable and did not decompose until 600 K. Above 600 K, the Nb-ethoxide species was dehydrated to ethene and water as shown in Fig. 5. On the other hand, when the Nb-ethoxide intermediate was exposed to ethanol, the dehydrogenation of ethanol proceeded at much lower temperatures such as 423 K, with ca. 100% selectivity. Thus the switchover of the reaction path from dehydration (γ-CH bond break) to dehydrogenation (β-CH bond break) by the second ethanol molecule weakly adsorbed on the Nb-ethoxide (**13**) is observed (Fig. 5). Even if an adsorbed species at the surface is too stable in vacuum or before catalysis, the catalytic reaction is able to proceed through the same species by activation of the intermediate by the reactant [3,4]. Thus, it may be critical for the dehydrogenation on Nb sites

Table 2
Catalytic performance of the Nb monomer, dimer, and monolayer supported on SiO_2, and an impregnation Nb catalyst for dehydrogenation and dehydration (intra and inter) of ethanol[a]

Catalyst	Initial rate (mmol min^{-1} (g Nb)$^{-1}$)			Selectivity (%)		
	Total	AA	E + DE	AA	E	DE
Monomer[b]	1.25	1.20	0.049	96.1	2.8	1.1
Dimer[b]	0.18	0.004	0.176	2.1	24.2	73.7
Monolayer[c]	0.11	0.001	0.106	0.9	99.1	0.0
Impregnated[b]	0.17	0.052	0.118	30.5	20.2	49.3

[a] AA: acetaldehyde, E: ethene, DE: diethyl ether, ethanol: 3.1 kPa.
[b] 523 K.
[c] 573 K.

to create a vacant site with an appropriate conformation for the transition state on which electron donation-induced activation of β-hydrogen of the C_2H_5O group is favorable.

The weakly adsorbed ethanol molecules, which can exist at the catalyst surface only in the presence of gas phase ethanol, play an important role in the surface catalytic dehydrogenation. Similar promoting effects of weakly adsorbed molecules have been observed in water gas shift reactions on MgO, ZnO, and Rh/CeO_2 [2–4]. Further, we have found that impinging molecules under catalytic reaction conditions play a crucial role in surface catalytic reactions even if the adsorption of 'promoter' is undetectable at the catalyst surface. NO decomposition on Co/Al_2O_3 catalyst proceeded via Co-dinitrosyl species ($Co(NO)_2$), where CO molecules that were undetectable at the catalyst surface promoted remarkably the reactivity of the $Co(NO)_2$ species at the surface by changing the conformation and increasing the amount of dinitrosyls [3,4]. From these results, a new aspect of catalysis "surface catalytic reactions assisted by gas phase molecules" has been presented [2–4].

The Nb dimer/SiO_2 catalyst (**2**) showed high selectivity for the dehydration of ethanol irrespective of the presence or absence of the ambient ethanol (Table 2). The dehydrogenation observed on the Nb monomer catalyst was remarkably suppressed to 1/300 and the dehydration was promoted by four times on the dimer (**2**), indicating that the Nb dimers on SiO_2 have an acidic character. It is to be noted that the change of the number of Nb atoms at the active sites from one to two metal atoms gives rise to a complete reverse of basicity/acidity in the catalytic properties. In the dimer (**2**), the access of a second ethanol molecule to the Nb atom coordinated with a first ethanol molecule in a preferable conformation is difficult unlike the case of the monomer (**1**). Furthermore, the Lewis acidity of the Nb atoms in the dimer (**2**) is increased by the oxygen bridge.

The monolayer (**3**) was active and selective for C_2H_4 formation from C_2H_5OH in the temperature range 423–573 K as shown in Table 2. The monolayer catalyst (**3**) always showed the selective intramolecular dehydration of ethanol, suggesting that the Lewis acid sites in the monolayer niobium oxides may be distributed in an isolated manner. The niobium oxide layer is somewhat distorted by the structural mismatch and the strong Nb–O–Si interaction between the Nb oxide overlayer and the SiO_2 surface as proven by EXAFS. The distortion and mismatch should be released by the creation of Lewis-acidic Nb sites. Nb-oxide monolayers on various oxide supports have been extensively investigated and characterized by Raman spectroscopy [24]. These structures are described as being made up of an octahedrally coordinated NbO_6 structure with different degree of distortion. The Lewis acid sites may be dispersed basically at the NbO_6 overlayer. This type of catalyst is applicable to intramolecular dehydration processes.

3.2. Rh catalysts

The catalytic activities of Rh_2/SiO_2 (**4**), Rh_2/TiO_2 (**6**), Rh_2/Al_2O_3 (**8**) and Rh_2/MgO (**9**) for ethene hydroformylation are compared in Table 3 [19,20]. Compared with a conventional impregnated Rh catalyst, only Rh_2/SiO_2 (**4**) showed activity and selectivity

Table 3
TOF and selectivity of ethene hydroformylation at 413 K[a]

Catalyst	TOF (10^{-4} molecules Rh^{-1} min^{-1})			Selectivity (%)
	Total	Ethane	Propanal	
Impregnated Rh/SiO_2	22.8	21.5	1.3	5.6
Rh_2/SiO_2	36.9	4.1	32.8	88.9
Rh_2/SiO_2[b]	268.0	133.0	135.0	50.2
Rh_2/TiO_2	6.3	6.3	0	0
Rh_2/Al_2O_3	6.8	6.8	0	0
Rh_2/MgO	56.0	56.0	0	0

[a] $CO:H_2:C_2H_4 = 1:1:1$ (total pressure = 40.0 kPa).
[b] $CO:H_2:C_2H_4 = 0.2:1:1$ (total pressure = 33.3 kPa).

for the hydroformylation at reduced pressures around 400 K, and the other catalysts were all inactive. The activity of the impregnated Rh catalyst for propanal formation was very slow and the selectivity was as low as 5.6%. Under the identical conditions, for the Rh dimer catalyst (**4**), the formation of propanal was remarkably promoted. The turnover frequency (TOF) for the propanal formation was 30 times larger than that for the impregnation catalyst. Furthermore, the selectivity of the hydroformylation was found to be 88.9% which is much higher than 5.6% for the impregnation catalyst. When the reaction rate was increased to about 100 times, the selectivity was still as high as 50.2%. It corresponds well to the CO insertion reaction promoted by Rh–Rh bonding observed by FT-IR and EXAFS [19]. On Rh_2/SiO_2 (**4**), CO insertion proceeds in conjunction with the formation of the Rh–Rh bond as shown in Fig. 2.

Hydroformylation reaction of alkenes is known to proceed on mono-metal site like mononuclear metal complexes in homogeneous systems. However, mono-metal sites are generally less active in heterogeneous systems. For supported Rh catalysts, the activity shows a maximum rate at an optimum metal particle size. In contrast to homogeneous reaction systems, surfaces Rh clusters or small particles are more active than Rh monomers, suggesting an important metal–metal interaction at the supported Rh catalysts. To examine the reason why the Rh dimer on SiO_2 is so selective, we characterized the structures of the Rh dimer (**4**) in the course of the catalytic reaction by EXAFS. When the dimer (**4**) was exposed to CO, dicarbonyls (**5**) were formed and simultaneously the Rh–Rh bond was broken. The species (**5**) was transformed to the acyl species (**4**) again by heating at 423 K, accompanied with rebonding of Rh–Rh. By CO adsorption, the dicarbonyls (**5**) appeared again and the Rh–Rh bond was broken (Fig. 2). The transformation between the two structures was reversible. The acyl group on Rh reacted with H_2 to form propanal. Ethene adsorbs, followed by CO adsorption and CO insertion, then the species (**4**) is regenerated. Catalytic hydroformylation reaction proceeds by the cycle involving CO adsorption, CO insertion and reaction with hydrogen in conjunction with the reversible formation and breaking of the Rh–Rh bond [19].

Chemistry of the dimer is different from chemistry of the monomer. As known in homogeneous systems, on Rh monomers CO insertion to alkyl to form acyl species can proceed only in the presence of additional extra CO as shown in Fig. 2. However, on the Rh dimer (**4**), the presence of extra CO decomposes the acyl species to the dicarbonyls. The CO insertion can proceed without aid of extra CO on the dimers supported on SiO_2 as shown in Fig. 2. The direction is opposite to each other. The catalytic ethene hydroformylation on Rh_2/SiO_2 is referred to metal-assisted catalysis by the two adjacent Rh atoms.

On Rh_2/TiO_2, the Rh–Rh bond was also regenerated by heating the dicarbonyl species (**7**) in Fig. 3, but it was accompanied by the formation of CO-bridged species (**6**), where one of the dicarbonyl ligands was merely desorbed [20]. Thus the CO insertion promoted by Rh–Rh bond formation in Fig. 2 did not take place on Rh_2/TiO_2 as shown in Fig. 3.

We were not able to observe a Rh dimer structure by EXAFS as main species on Rh_2/Al_2O_3 (**8**). Rh atoms were attached as monomers at the Al_2O_3 surface as shown in Fig. 3. The Rh monomer species showed little CO insertion ability [20]. MgO-supported Rh species was aggregated to form a small Rh cluster with direct Rh–O bonding [20]. The Rh–Rh bonding in the cluster was stable and not cleaved by exposure to CO. The metal-assisted CO insertion was not observed with the Rh_2/MgO catalyst either.

3.3. Molecular imprinting catalysts

A goal of molecular imprinting is to create solid materials containing chemical functionalities that are spatially organized by chemical interactions with template molecules during the synthesis process. Subsequent removal of the template molecules leaves behind designed sites for the recognition of template-analog molecules. The materials thus obtained ideally suit for applications to various technologies such as separation, medical diagnostics, drug delivery, chemical sensing and catalysis.

Katz and Davis [10] reported preparation procedures to create the imprinted silicas. The obtained silica matrix was characterized to have 0.8–1.0 nm pore size. The molecular imprinted silica was used as a base catalyst for the Knoevenagel condensation reaction of malononitrile with isophthalaldehyde. Fache et al. [11] applied polymer-matrix molecular imprinting catalysts with Rh complexes to asymmetric

hydrogenation by hydrogen transfer between phenylmethylketone and isopropanol. The obtained catalyst showed much higher ee% selectivities than Rh complex catalysts without the template molecule. Morihara et al. [13] reported a pioneering work on footprint catalysts prepared by incorporation of Al^{3+} and loading of template molecules in silica matrix, which were applied to butanolysis of benzoic anhydride. In spite of many challenges, the formation of substrate-specific cavities within bulk silicas and polymers has been difficult to accomplish experimentally, though the molecular imprinting is conceptually straightforward.

Niwa and coworkers [25,26] prepared imprinted materials by masking SnO_2 surface by SiO_2 overlayers. The obtained catalysts were applied as a chemical sensor which distinguishes the shape of gas molecules. Unfortunately, these catalysts have not been characterized well, and the reason of generation of the selectivity is not clear at present.

We have prepared a variety of oxide monolayers on SiO_2, ZSM-5, etc. to develop new type of surface materials with unique catalytic performances by chemical reactions of precursor complexes with surface OH groups of oxide supports [27–32]. The surface reaction technique using alkoxides as precursors has successfully been applied to the synthesis of oxide monolayers with well-defined structures, for example, ZrO_2/ZSM-5 [28], Nb_2O_5/SiO_2 [29], TiO_2/SiO_2 [30], and GeO_2/SiO_2 [31]. These materials have also been employed as supports for Pt [30] and Rh [32].

By combining and extending the previous two different preparation techniques for the attached metal complexes and oxide overlayers on oxide-support surfaces, we have synthesized new surface-imprinted catalysts for ester hydrolysis [16,21] and alkene hydrogenation [22,23]. Fig. 6 shows *t*-plots for the molecular imprinting catalyst (**10**) and the supported catalyst (**11**) without template molecules. In the isotherms for

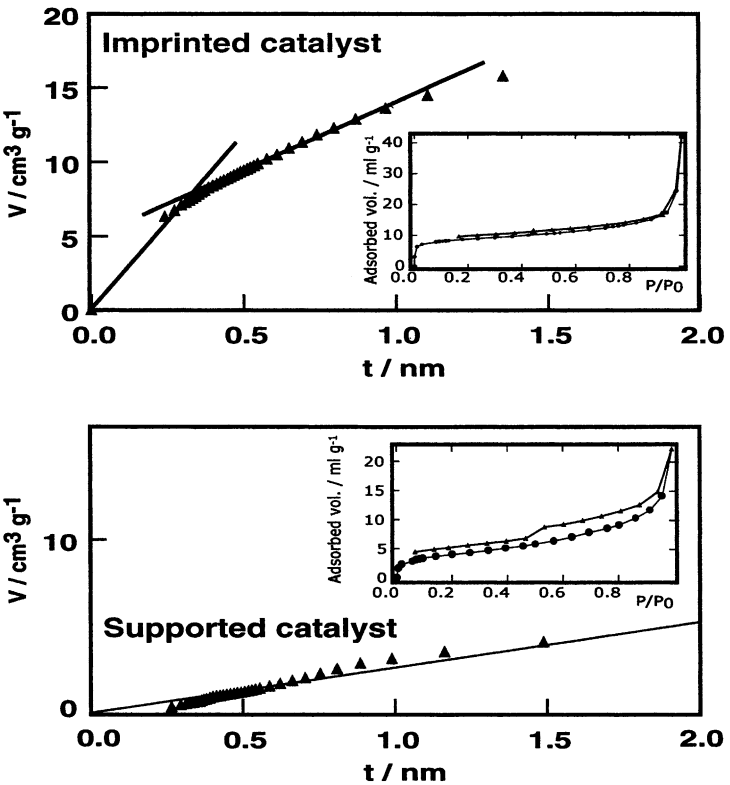

Fig. 6. *t*-Plots for N_2 adsorption on the imprinted catalyst (**10**) and the supported catalyst (**11**).

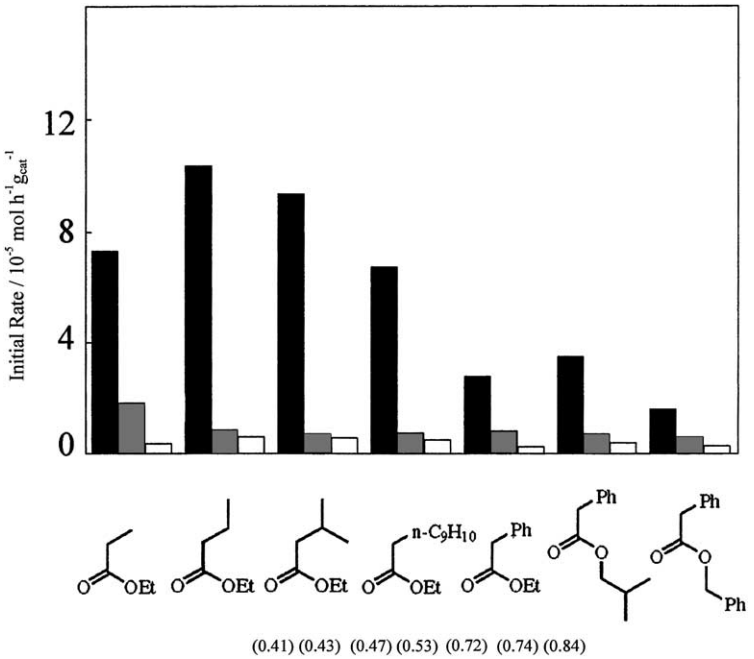

Fig. 7. Initial rates of the hydrolysis of various esters with different molecular cross-sections (values in parentheses) on the imprinted catalyst (**10**) (filled), the supported catalyst (**11**) (shaded), and α-alumina (open).

the catalyst (**10**), little hysteresis was observed and the shape of the isotherm was assigned to type 2 classification for pore materials. The result suggests that there are micropores on the surface of the catalyst (**10**). On the contrary, a hysteresis was observed above relative pressure of 0.5 in the catalyst (**11**), and the shape of the isotherm is assigned to type 4 classification. The result implies that mesopores also exist on the surface of the catalyst (**11**). The analysis demonstrates that micropores with diameter around 0.76 nm and with depth of about 1.2 nm were produced on the alumina by the molecular imprinting method.

The molecular imprinting catalyst (**10**) was used as catalyst for the hydrolysis of esters such as ethyl propionate, ethyl butyrate, ethyl isobutyrate, ethyl decanoate, ethyl phenylacetate, isobutyl phenylacetate, and benzyl phenylacetate. The initial rates of the ester hydrolysis reactions are shown in Fig. 7. For comparison, the initial rates of the reactions on the supported catalyst (**11**) and the α-alumina are also shown in Fig. 7. The hydrolysis of ethyl propionate, ethyl butyrate, ethyl isobutyrate, and ethyl decanoate was much faster than the hydrolysis of ethyl phenylacetate, isobutyl phenylacetate, and benzyl phenylacetate. The results demonstrate a shape selectivity for the molecular imprinting catalyst (**10**).

The molecular size of the diethyl benzyl phosphonate template molecule is estimated to be 0.72 nm^2. However, the hydrolysis of ethyl phenylacetate with a similar size to the template molecule size was slower among the reactants used in this study as shown in Fig. 7. The cavity size produced by the imprinting technique was 0.76 nm, which corresponds to about 0.5 nm^2 cross-section. The results in Fig. 7 show a critical cross-section of the reactant molecules at 0.53 nm^2 for the catalytic reaction, which coincides with the imprinting cavity dimension. In regard to the difference between the template size and the cavity size, the reason is not clear at present, but the present imprinting technique seems to provide a uniform pore size in the SiO_2 overlayers.

The activation energy for the molecular imprinting catalyst (**10**) was 12 kJ mol^{-1}, while the activation energy for the supported catalyst (**11**) prepared without

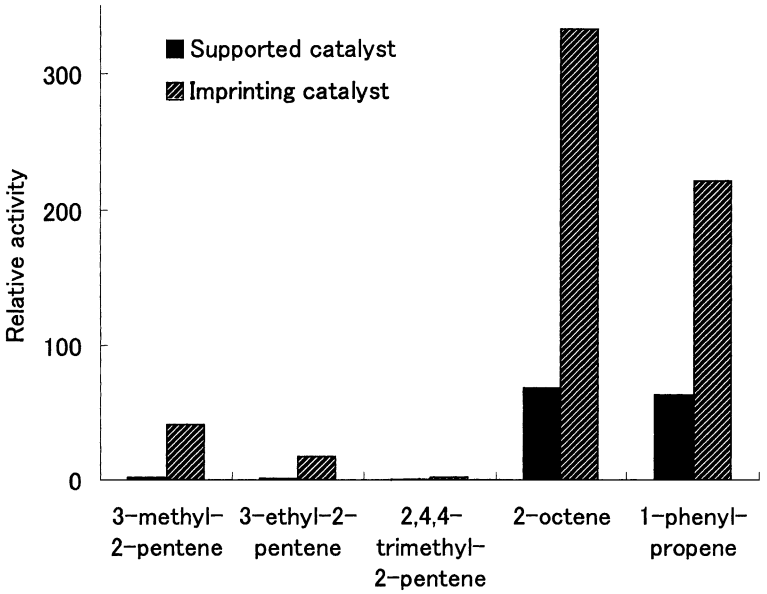

Fig. 8. Relative activities of the imprinted Rh catalyst and the supported Rh catalyst for the hydrogenation of various alkenes at 348 K. Relative activities: the initial rates referred to the initial rate of the 3-ethyl-2-pentene hydrogenation on the supported catalyst.

the template was 79 kJ mol^{-1}. The difference is very large; the former is much smaller than the latter which is similar to the value of usual acidic catalysis for ester hydrolysis. The acid sites produced in the presence of the template molecules were more active than those produced in the absence of the template molecules. Probably, the acidic sites are created at the interface between the alumina surface and the silica overlayers in the imprinting cavity because it is known that Brönsted acid sites are formed at the boundary of silica and alumina at elevated temperatures. The acid strength may be affected by the arrangement of the interface in the cavity. Further, the activation entropy was -312 J mol^{-1} K^{-1} for the molecular imprinting catalyst (**10**), while it was about -50 J mol^{-1} K^{-1} for the supported catalyst (**11**). The large minus activation entropy value observed with the imprinting catalyst (**10**) is similar to that for enzymatic reactions which occur on active centers located in the enzyme cavity. In the molecular imprinting catalyst (**10**), the reaction intermediate/the transition state may be stabilized in the molecular cavity with restriction of the motion of the intermediate.

Fig. 8 shows the relative activities of the imprinted and supported Rh catalysts (the ratio of initial rates) for the hydrogenation of 3-methyl-2-pentene, 3-ethyl-2-pentene, 2,4,4-trimethyl-2-pentene, 2-octene, and 1-phenylpropene at 348 K, where the initial rates for the hydrogenation were referred to the initial rate of the 3-ethyl-2-pentene hydrogenation on the supported Rh catalyst. The analog complex $RhCl(P(OCH_3)_3)_3$ in a homogeneous system was inactive under similar reaction conditions. It is to be noted that the imprinted catalyst was tremendously active compared to the supported catalyst. In other words the catalytic activity of the Rh complexes in the cavity of the SiO_2-overlayer matrix on SiO_2 surface is remarkably promoted as compared with the supported Rh complexes before the matrix preparation by the CVD technique. As far as we know, the finding of the high promoting effect of the SiO_2-overlayer matrix is the first in molecular imprinting catalysts with metal complexes as active sites reported to date. The selectivity of the imprinted catalyst for the alkene hydrogenation was also different from that of the supported catalyst. Preliminary EXAFS study indicated the formation of new Rh dimer complex which could be produced in the cavity of SiO_2-overlayer matrix. Ugo et al. [33] reported the synthesis of dinuclear (silyloxy)rhodium complexes with Rh–Rh bond

distances of 0.2785 and 0.2922 nm from $Rh_2Cl_2(CO)_4$ in solution. However, our novel surface Rh dimer in the cavity is suggested to have a different structure with a much shorter Rh–Rh distance around 0.269 nm [23]. The detail of the catalytic performance and characterization of the imprinted Rh sites will be reported separately [23].

References

[1] Y. Iwasawa, Adv. Catal. 87 (1987) 187.
[2] Y. Iwasawa, Proceedings of the 11th Congress on Catalysis, Baltimore, MD, Stud. Surf. Sci. Catal. 101 (1996) p. 21
[3] Y. Iwasawa, Acc. Chem. Res. 30 (1997) 103.
[4] T. Shido, A. Yamaguchi, K. Asakura, Y. Iwasawa, J. Mol. Catal. A 163 (2000) 67.
[5] B.C. Gates, L. Guczi, H. Knözinger (Eds.), Metal Cluster in Catalysis, Elsevier, Amsterdam, 1986.
[6] M. Chabanas, A. Baudouin, C. Coperet, J.-M. Basset, J. Am. Chem. Soc. 123 (2000) 2062.
[7] A. Yamaguchi, K. Asakura, Y. Iwasawa, J. Mol. Catal. A 146 (1999) 65.
[8] Y. Izumi, T. Chihara, H. Yamazaki, Y. Iwasawa, J. Phys. Chem. 98 (1994) 594.
[9] D.I. Kondarides, K. Tomishige, Y. Nagasawa, U. Lee, Y. Iwasawa, J. Mol. Catal. A 111 (1996) 145.
[10] A. Katz, M.E. Davis, Nature 403 (2000) 286.
[11] F. Fache, B. Dunjic, P. Gamez, M. Lemaire, Topics Catal. 4 (1997) 201.
[12] C. Yu, K. Mosbach, J. Org. Chem. 62 (1997) 4057.
[13] K. Morihara, S. Kurihara, J. Suzuki, Bull. Chem. Soc. Jpn. 61 (1988) 3991.
[14] G. Wulff, Angew. Chem. Int. Ed. Engl. 34 (1995) 1812.
[15] W.F. Maier, J.A. Martens, S. Klein, J. Heilmann, R. Parton, K. Vercruysse, P.A. Jacobs, Angew. Chem. Int. Ed. Engl. 35 (1996) 180.
[16] A. Suzuki, T. Shido, Y. Iwasawa, Shokubai (Catalysts and Catalysis) 43 (2001) 119.
[17] K. Fukui, S. Sugiyama, Y. Iwasawa, Phys. Chem. Chem. Phys. 3 (2001) 3871.
[18] N. Ichikuni, K. Asakura, Y. Iwasawa, J. Chem. Soc., Chem. Commun. (1991) 112.
[19] K. Asakura, K.K. Bnado, Y. Iwasawa, H. Arakawa, K. Isobe, J. Am. Chem. Soc. 112 (1990) 9096.
[20] K.K. Bando, K. Asakura, H. Arakawa, K. Isobe, Y. Iwasawa, J. Phys. Chem. 100 (1996) 13636.
[21] A. Suzuki, M. Tada, T. Sasaki, T. Shido, Y. Iwasawa, in press.
[22] M. Tada, T. Sasaki, T. Shido, Y. Iwasawa, Proceedings of 10th International Symposium on Homogenous Heterogeneous Catalyst, SHHC 10, Lyon, 2001, p. 155 (Abstract).
[23] M. Tada, T. Sasaki, T. Shido, Y. Iwasawa, in press.
[24] J.M. Jehng, I.E. Wachs, J. Phys. Chem. 95 (1991) 7373.
[25] N. Katada, T. Tanimura, M. Niwa, Shokubai (Catalysts and Catalysis) 41 (1999) 480.
[26] N. Kadakari, N. Katada, M. Niwa, Adv. Mater. CVD 3 (1997) 59.
[27] Y. Iwasawa, Tailored Metal Catalysts, Reidel, Dordrecht, 1986.
[28] K. Asakura, M. Aoki, Y. Iwasawa, Catal. Lett. 1 (1988) 395.
[29] M. Shirai, K. Asakura, Y. Iwasawa, J. Phys. Chem. 95 (1991) 9999.
[30] K. Asakura, J. Inukai, Y. Iwasawa, J. Phys. Chem. 96 (1992) 829.
[31] K. Okumura, K. Asakura, Y. Iwasawa, Langmuir 14 (1998) 3607.
[32] K. Okumura, K. Asakura, Y. Iwasawa, Catal. Today 39 (1998) 343.
[33] R. Ugo, R. Psaro, A. Sironi, M. Moret, C. Zucchi, F. Ghelfi, G. Palyi, Inorg. Chem. 33 (1994) 4600.